Vol 16 No 4, April 2007
1009-1963/2007/16(04)/1031-07

Chinese Physics

© 2007 Chin. Phys. Soc.
and IOP Publishing Ltd

Analysis of the far spatial coherent suppressed single peak field distribution of a rectangular wave-guide laser

Wu Xing-Fei(吴行飞)†, Yang Jing(杨 静), and Xin Jian-Guo(辛建国)

Department of Optical Engineering, Beijing Institute of Technology, Beijing 100081, *China*

(Received 9 June 2006; revised manuscript received 27 October 2006)

A theory of the far spatial coherent-suppressed single-peak field distribution of a rectangular wave-guide CO_2 laser is presented. The theoretical analysis shows that a rectangular wave-guide laser can have an output intensity distribution in far field similar to that produced from a wave-guide array laser, which is in agreement with the experimental result. A single-peak mode output is obtained within 5 metres. The experimental far-field spread angle in the bigger-Fresnel number direction is 0.63 mrad, compared to the calculated one, 0.6 mrad, and when the length of the laser resonator is changed, a double-peak or multi-peak in far-field distribution of the laser is obtained.

Keywords: wave-guide array,CO_2 laser, field distribution
PACC: 4255D，4260D，4260F

To obtain a far suppressed single-peak field distribution in a RF-excited CO_2 laser, much research work has been conducted.[1−7] In a rectangular waveguide laser, whose waveguide can have different sizes and Fresnel numbers in the two transverse directions, the smaller Fresnel number N will keep $N < 1$, while the bigger Fresnel number will keep $N > 1$, even $N \gg 1$. In the traditional waveguide laser resonator theory, a hollow rectangular waveguide is supposed to have infinite length with definite transverse dimensions, and the mode of the hollow rectangular waveguide laser resonator can be described by the waveguide mode function.[8,9]

According to the traditional hollow waveguide laser resonator theory, the output mode of a rectangular waveguide laser should be a high-order mode or multi-mode of high orders, the far-field intensity distribution of which should be double-peak or multi-peak, but some experimental results have shown that a rectangular waveguide CO_2 laser can produce the result of a single-peak field distribution.[10] It has been seen that the traditional waveguide resonator theory cannot well explain the experimental results of the spatially suppressed single peak of the intensity distribution. Therefore, in this paper, a theory called quasi-waveguide resonator theory is put forward, the output mode of the quasi-waveguide resonator is analysed, and the experimental results are in good agreement with the results predicted by the proposed theory.

In practice, the rectangular waveguide laser used consists of a total reflection mirror, an output mirror and a section of rectangular waveguide which has a finite length and the transverse dimensions of $a \times b$ as shown in Fig.1. A roundtrip of the light wave in this resonator includes two trips through the guide and the propagation to and from the two resonator mirrors through the free-space. In the absence of a waveguide, the free-space resonator mode structure and characteristics could be described by free-space resonator theory. When a waveguide is present, the effect of the waveguide will play an important role in forming the stable axial and transverse mode structure of the resonator. Due to the combination effect of waveguide and free-space propagation in the quasi-waveguide resonator, the mode of the resonator will not be a pure waveguide mode or a pure free-space resonator mode. These characteristics make it inappropriate to describe the quasi-waveguide resonator modes with free-space resonator theory and the traditional waveguide resonator theory. The propagation of electromagnetic field in the quasi-waveguide resonator is illustrated in Fig.2. Inside the waveguide, from M_1 to M_2 or from M_2 to M_1, the electromagnetic field is influenced not only by the waveguide aperture but also the waveguide wall reflection effect. While outside the waveguide, from M_1 to M_0 or from M_2 to M_3, the electromagnetic field propagates in the free space.

†E-mail: bitxfw@sohu.com

The diffraction loss in the quasi-waveguide resonator is lower than that in the waveguide resonator. The free space between the waveguide aperture and the resonator mirror makes the coupling loss different in different mode, which characterizes the output mode of the quasi-waveguide laser. This property of the mode produced by the rectangular quasi-waveguide laser is analysed by using the numerical approach.

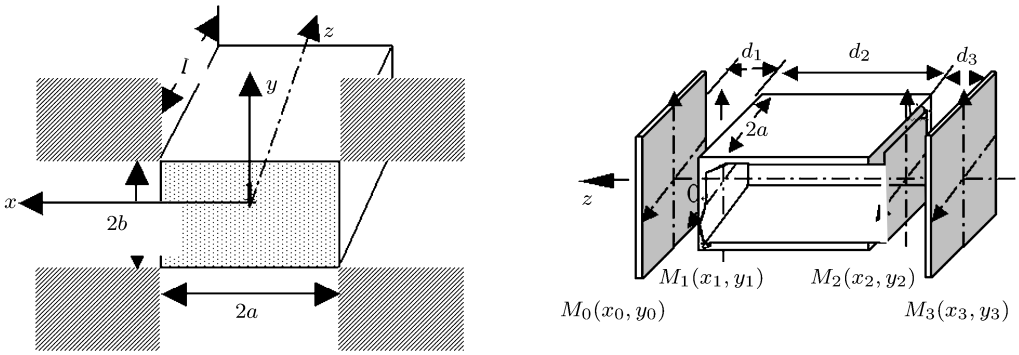


Fig.1. Diagram of the rectangular waveguide resonator.

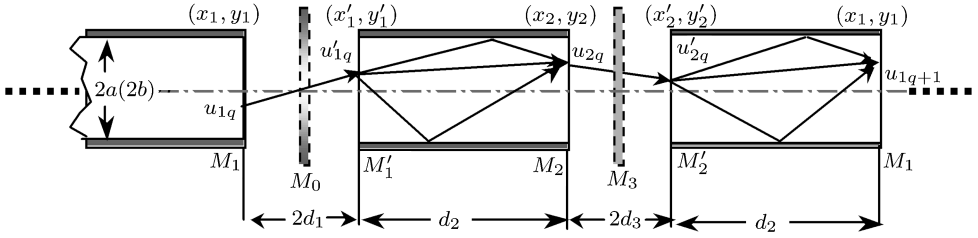


Fig.2. Diagram of the simplified model of light wave diffraction process.

The field distributions on resonator mirrors M_0, M_3 and waveguide apertures M_1, M_2 are $u_o(x_o, y_o)$, $u_3(x_3, y_3)$ and $u_1(x_1, y_1)$, $u_2(x_2, y_2)$ respectively in the plane-parallel quasi-waveguide resonator illustrated in Fig.1. Because the flat mirror has no effect on the curvature of the propagation wave front, the field propagation in the resonator can be modelled by the physical picture as shown in Fig.2, It can be seen that after a round trip of propagating through the distance of $2d_1$ in free space, passing through the waveguide d_2, propagating the distance $2d_3$ in free space to reach the plane of M_2' and going back along the same path to the plane of M_1, the starting field $u_1(x_1, y_1)$ becomes $u_1'(x_1', y_1')$. After q round trips of propagation, for the steady field distribution, the field on the mirrors can be expressed as:

$$u_{1q+1} = \gamma u_{1q}, \tag{1}$$

$$u_{2q+1} = \gamma u_{2q}, \tag{2}$$

where γ is the propagation constant, denoting the phase shift and amplitude attenuation.

Equations (1) and (2) show the steady field equations or the eigen equations in the cavity. When the polarization of the light is taken into consideration, Eqs.(1) and (2) can be rewritten as

$$\begin{aligned} u_{1q}(x_1, y_1) &= u_{1qp}(x_1, y_1)p + u_{1qs}(x_1, y_1)s, \\ u_{2q}(x_2, y_2) &= u_{2qp}(x_2, y_2)p + u_{2qs}(x_2, y_2)s, \\ u'_{1q}(x'_1, y'_1) &= u'_{1qp}(x'_1, y'_1)p + u'_{1qs}(x'_1, y'_1)s, \\ u_{2q}(x'_2, y'_2) &= u_{2qp}(x'_2, y'_2)p + u_{2qs}(x'_2, y'_2)s, \\ & \qquad q = 0, 1, 2, \ldots, \end{aligned} \tag{3}$$

where $u_{1qp}(x_1, y_1)$, $u_{2qp}(x_2, y_2)$, $u'_{1qp}(x'_1, y'_1)$, $u'_{2qp}(x'_2, y'_2)$ and $u_{1qs}(x_1, y_1)$, $u_{2qs}(x_2, y_2)$, $u'_{1qs}(x'_1, y'_1)$, $u'_{2qs}(x'_2, y'_2)$ are the p components and s components of the wave field distribution. The propagation of the field can be described by the following equations:

$$u'_{1qp}(x'_1, y'_1) = \frac{-\mathrm{i}}{\lambda} \iint\limits_{2a \times 2b} \frac{\mathrm{e}^{-\mathrm{i}k}\rho_1}{\rho_1} u_{1qp}(x_1, y_1)\mathrm{d}x_1\mathrm{d}y_1,$$

$$
\begin{aligned}
u'_{1qs}(x'_1,y'_1) = & \frac{-\mathrm{i}}{\lambda}\iint\limits_{2a\times 2b}\frac{\mathrm{e}^{-\mathrm{i}k}\rho_1}{\rho_1}u_{1qs}(x_1,y_1)\mathrm{d}x_1\mathrm{d}y_1,\\
u_{2qp}(x_2,y_2) = & \frac{-\mathrm{i}}{\lambda}\iint\limits_{2a\times 2b}u'_{1qp}(x'_1,y'_1)\Bigg(\frac{\mathrm{e}^{-\mathrm{i}k\rho_{20}}}{\rho_{20}}+\Bigg(\frac{\mathrm{e}^{-\mathrm{i}k\rho_{2A1}}}{\rho_{2A1}}r_{Ap1}+\frac{\mathrm{e}^{-\mathrm{i}k\rho_{2A2}}}{\rho_{2A2}}r_{Ap2}\Bigg)\\
& +\Bigg(\frac{\mathrm{e}^{-\mathrm{i}k\rho_{2C1}}}{\rho_{2C1}}r_{Cs1}+\frac{\mathrm{e}^{-\mathrm{i}k\rho_{2C2}}}{\rho_{2C2}}r_{Cs2}\Bigg)\Bigg)\mathrm{d}x'_1\mathrm{d}y'_1,\\
u_{2qs}(x_2,y_2) = & \frac{-\mathrm{i}}{\lambda}\iint\limits_{2a\times 2b}u'_{1qs}(x'_1,y'_1)\Bigg(\frac{\mathrm{e}^{-\mathrm{i}k\rho_{20}}}{\rho_{20}}+\Bigg(\frac{\mathrm{e}^{-\mathrm{i}k\rho_{2A1}}}{\rho_{2A1}}r_{As1}+\frac{\mathrm{e}^{-\mathrm{i}k\rho_{2A2}}}{\rho_{2A2}}r_{As2}\Bigg)\\
& +\Bigg(\frac{\mathrm{e}^{-\mathrm{i}k\rho_{2C1}}}{\rho_{2C1}}r_{Cp1}+\frac{\mathrm{e}^{-\mathrm{i}k\rho_{2C2}}}{\rho_{2C2}}r_{Cp2}\Bigg)\Bigg)\mathrm{d}x'_1\mathrm{d}y'_1,\\
u_{1qp}(x_1,y_1) = & \frac{-\mathrm{i}}{\lambda}\iint\limits_{2a\times 2b}u'_{2qp}(x'_1,y'_1)\Bigg(\frac{\mathrm{e}^{-\mathrm{i}k\rho_{20}}}{\rho_{20}}+\Bigg(\frac{\mathrm{e}^{-\mathrm{i}k\rho_{2A1}}}{\rho_{2A1}}r_{Cp1}+\frac{\mathrm{e}^{-\mathrm{i}k\rho_{2A2}}}{\rho_{2A2}}r_{Cp2}\Bigg)\\
& +\Bigg(\frac{\mathrm{e}^{-\mathrm{i}k\rho_{2C1}}}{\rho_{2C1}}r_{Cs1}+\frac{\mathrm{e}^{-\mathrm{i}k\rho_{2C2}}}{\rho_{2C2}}r_{Cs2}\Bigg)\Bigg)\mathrm{d}x'_2\mathrm{d}y'_2,\\
& q=0,1,2,\ldots, \qquad (4)
\end{aligned}
$$

In the above, r_{Api}, r_{Cpi} $(i=1,2)$ are the reflectivities of p component wave reflected by aluminium surface and ceramic surface respectively; and r_{Asi}, r_{Csi} $(i=1,2)$ are the reflectivities of s component wave; ρ_1 denotes the route of wave propagation from M_1 to M'_1, ρ_2 represents the route from M_1 (or M'_1 in Fig.2) to M_2 inside the waveguide, $\rho_2=\rho_{20},\rho_{2A1},\ \rho_{2A2},\rho_{2C1},\ \rho_{2C2},\rho_{20}$ is the route of the wave propagating from M_1 to M_2; ρ_{2A1},ρ_{2A2} and ρ_{2C1},ρ_{2C2} denote the routes of the wave inside the waveguide while reflected by the aluminium surface and ceramic surface respectively. The loss of the wave field increases with increasing number of reflections. In our calculation, we suppose that the electromagnetic field is reflected only one time on the surface in the waveguide before it passes through the waveguide, which is good enough for the accuracy of calculation.

According to Fresnel theory, the reflectivities of p component and s component of the incident wave can be written as:

$$
\begin{aligned}
r_p &= \frac{\mathrm{tg}(\theta_\mathrm{i}-\theta_\mathrm{d})}{\mathrm{tg}(\theta_\mathrm{i}+\theta_\mathrm{d})},\\
r_s &= -\frac{\sin(\theta_\mathrm{i}-\theta_\mathrm{d})}{\sin(\theta_\mathrm{i}+\theta_\mathrm{d})},
\end{aligned}
\qquad (5)
$$

where θ_i and θ_d denote the incident angle and refraction angle respectively. From the refractive law, we can obtain:

$$
\frac{\sin\theta_\mathrm{i}}{\sin\theta_\mathrm{d}}=\frac{k_l}{k_i}=\sqrt{\frac{\mu_2\varepsilon_2}{\mu_1\varepsilon_1}}=\sqrt{\mu_r\varepsilon_r}. \qquad (6)
$$

Here $\theta_\mathrm{d}, r_p, r_s$ can be determined by using $\varepsilon_r=5.5$–200, $\mu_r\approx 1$[11] (for ceramic), according to Eqs.(5) and (6). The reflection of the wave field from the conductive reflection surface can be described: for s component,

$$
r_s=\frac{(n_0k_0\cos\theta_\mathrm{i}-p)-\mathrm{i}q}{(n_0k_0\cos\theta_\mathrm{i}+p)+\mathrm{i}q}=\rho_\perp\exp(-\mathrm{i}\phi_\perp), \qquad (7)
$$

where n_0 is the refractive index of the medium in the waveguide and k_0 represents the propagation constant of wave in the medium.

In a good conductor, from $p\approx q\approx\eta k_o$ and $\eta\approx\sqrt{\sigma_2/(2\omega\varepsilon_0)}\gg 1$, we can obtain

$$
\begin{aligned}
\rho_\perp^2 &\approx \frac{(n_0k_0\cos\theta_\mathrm{i}-\eta)^2+\eta^2}{(n_0k_0\cos\theta_\mathrm{i}+\eta)^2+\eta^2}\approx 1-\gamma\cos\theta_\mathrm{i}, \qquad (8)\\
\tan\phi_\perp &\approx \frac{2n_0\eta q\cos\theta_\mathrm{i}}{(n_0\cos\theta_\mathrm{i})-2\eta^2}\approx -\gamma\cos\theta_\mathrm{i},\\
\gamma &= n_0/\eta\approx\sqrt{2\omega\varepsilon_1/\sigma_2}\ll 1. \qquad (9)
\end{aligned}
$$

The p component reflectance of the wave in a perfect conductor is

$$
r_p\approx\frac{(\cos\theta_\mathrm{i}-\gamma)-\mathrm{i}\cos\theta_\mathrm{i}}{(\cos\theta_\mathrm{i}+\gamma)-\mathrm{i}\cos\theta_\mathrm{i}}=\rho_{||}\exp(-\mathrm{i}\phi_{||}), \qquad (10)
$$

where

$$\rho_{||}^2 \approx \frac{(\cos\theta_{\rm i}-\gamma)^2+\cos^2\theta_{\rm i}}{(\cos\theta_{\rm i}+\gamma)^2+\cos^2\theta_{\rm i}}, \tag{11}$$

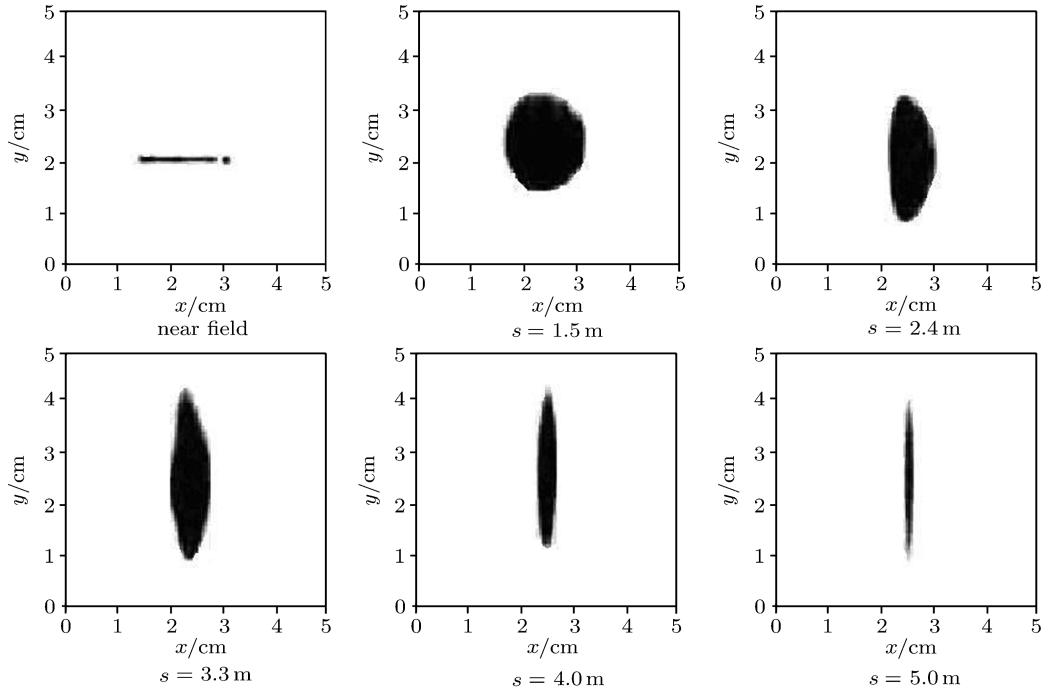
$$\tan\phi_{||} \approx \frac{2n_0k_0q\cos\theta_{\rm i}}{\gamma^2-2\cos^2\theta_{\rm i}}. \tag{12}$$

The reflectance calculation module of the metallic surface and ceramic surface in the waveguide can be obtained by using Eqs.(5)–(12).

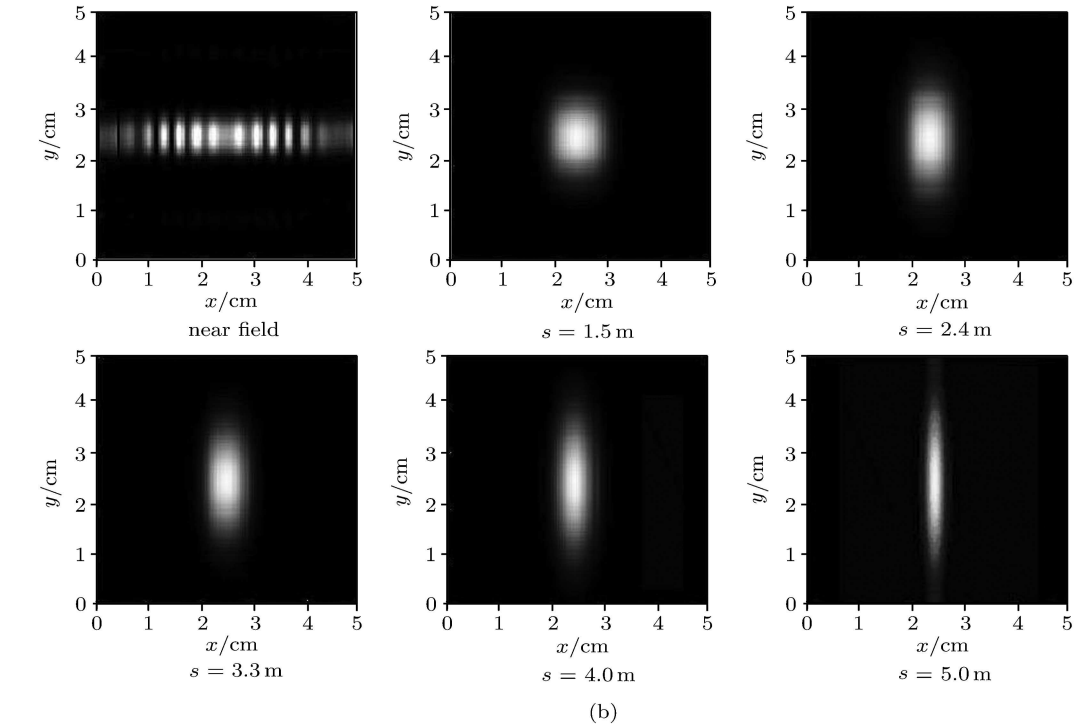
The near-field mode distribution of the experimental results is shown in Fig.3(a) and the far-field mode distributions of the experimental results are shown in Figs.3(a), 4(a) and 5(a). Our experiment is based on the plane-parallel waveguide resonator laser we have designed with the parameters (normal size): $2a = 20\,\text{mm}$, $2b = 1\,\text{mm}$, $d_2 = 200\,\text{mm}$, $d_1 = d_3 = 3\,\text{mm}$, $\lambda = 10.6\,\mu\text{m}$, the ceramic dielectric constant[4] ε_r=5.5; and the experimental mixture gas is CO_2:N_2:He_2(1:1:3) mixed with 5% Xe, the gas pressure being about $1.3\times10^4 \sim 2.7\times10^4\,\text{Pa}$, and the RF-excited frequencies being 70–110 MHz. The gas laser medium distribution has little influence on the laser output model because of the uniformity of the gas medium. Theoretical results are shown in Figs.3(b), 3(c), 4(b), 4(c), 5(b) and 5(c). Figures 3, 4 and 5 show the different results for different lengths of the laser resonator, which are in good agreement with the experimental results. The field mode has several nodes in x direction due to $N_x \gg 1$, while it has only 1 node in y direction due to $N_y < 1$. From the experimental and theoretical results, it can be seen that the output intensity distribution of the resonator field shows a line of spots in the near field and a spatially suppression in the far field in x direction.

The calculated and the experimental results of suppressed single-peak far-field distribution are shown in Fig.3, with the resonator parameters: $2a = 20\,\text{mm}$, $2b = 1\,\text{mm}$, $d_2 = 201.40\,\text{mm}$, the distances between resonator mirror and waveguide aperture $d_1 = 3.5\,\text{mm}$, $d_3 = 3.507\,\text{mm}$ and the laser wavelength $\lambda = 10.6\,\mu\text{m}$. A single-peak mode output is obtained within 5 metres using this resonator, and the experimental far-field spread angle in the bigger- Fresnel number direction is 0.63mrad, compared to the calculated one 0.6mrad. This means that the output light field has the characteristics which the array waveguide has. When the length of the laser resonator is changed, a double-peak or multi-peak in far-field distribution of the laser is obtained. The results are shown in Figs.4 and 5.

In conclusion, a new kind of quasi-waveguide theory is put forward in this paper, aiming to solve the difficulties confronted by the traditional waveguide laser resonator theory in explaining the characteristic of wide waveguide CO_2 laser output mode, based on the experimental studies of rectangular waveguide CO_2 laser; and the experimental results of the quasi-waveguide laser output mode are in good agreement with the theoretical ones.



(a)



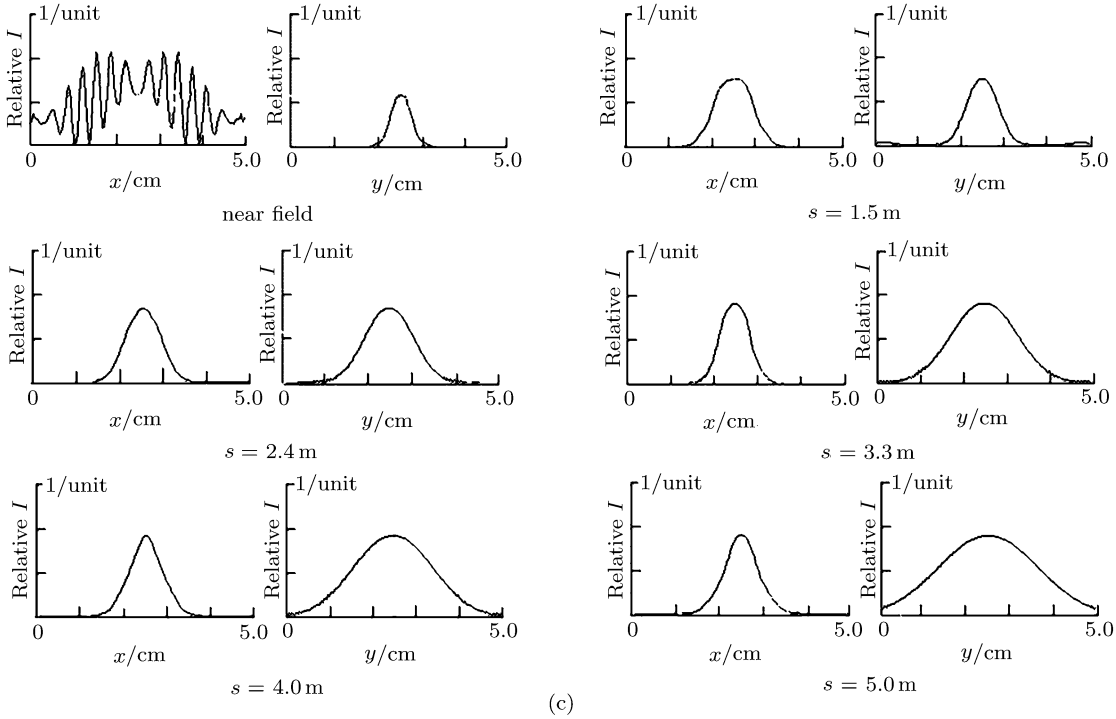


Fig.3. The single-peak distribution of output at different distances (the resonator length is 208.470 mm). (a) Experimental spots; (b) theoretical spots; (c) theoretical intensity distribution.

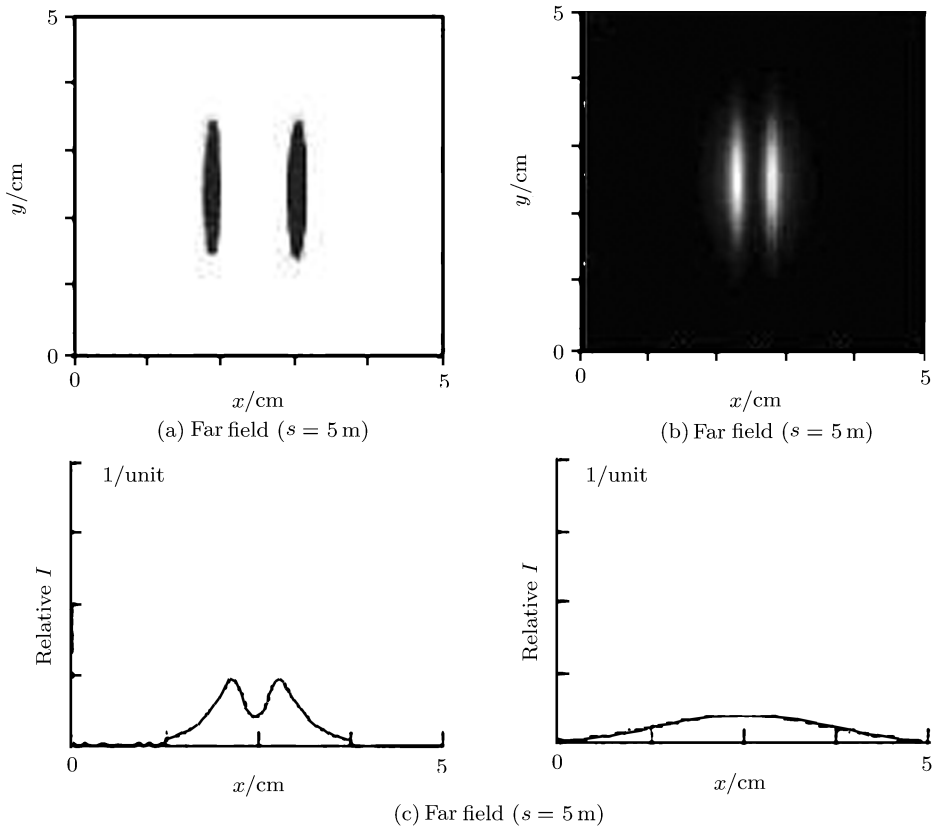


Fig.4. The double-peak field distribution of the output (the resonator length is 207.013 mm). (a) Experimental spots; (b) theoretical spots; (c) theoretical intensity distribution.

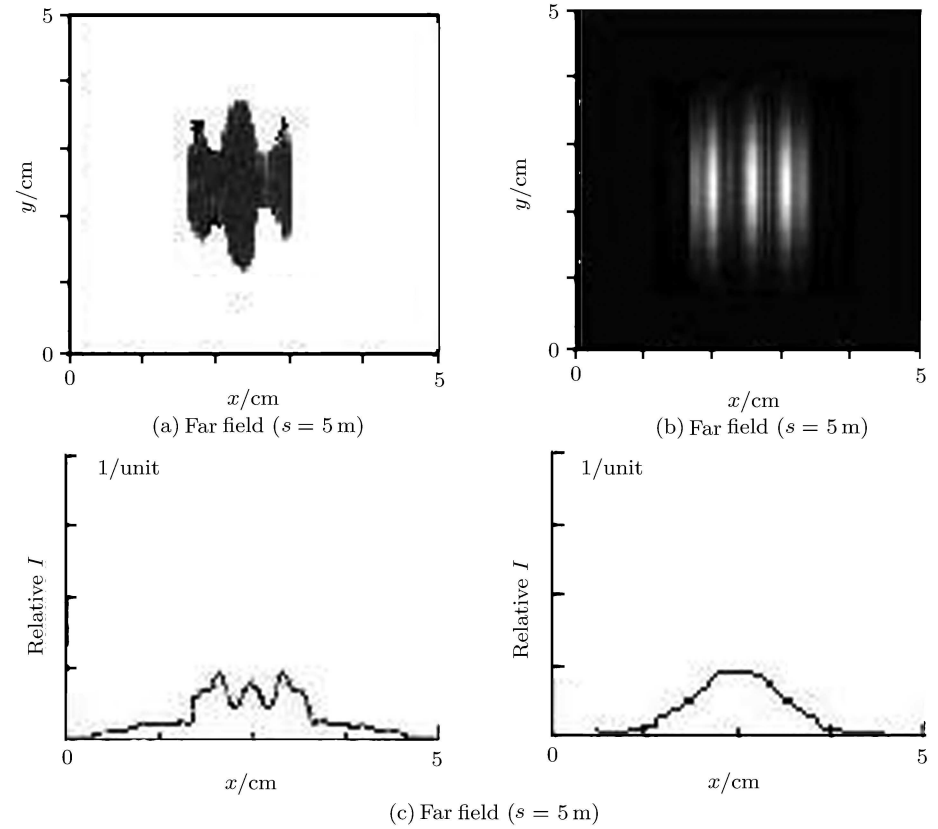


Fig.5. The multi-peaks field distribution of the output (the resonator length is 207.000 cm). (a) Experimental spots; (b) theoretical spots; (c) theoretical intensity distribution.

It is proved theoretically that the rectangular waveguide laser output mode may have double or multiple peaks in the far field, and in some situations a suppressed single-peak output field distribution, analogous to the one produced by array-waveguide laser, can be obtained, which is different from the one given by the traditional waveguide laser resonator theory. Quasi-waveguide laser theory given in this paper can be used to explain the double-peak or multi-peak far field characteristic and suppressed single-peak far field characteristic of the rectangular waveguide laser simultaneously, indicating that this theory is compatible to the traditional waveguide laser resonator theory. For an ideal waveguide, the quasi-waveguide laser resonator theory will change into the traditional laser resonator theory, and thus can well characterize a real wide waveguide laser.

References

[1] Jiao W T and Xin J G 1999 *Acta Phys. Sin.* **48** 1875 (in Chinese)

[2] Hussain Badran 2004 *Chin. Phys.* **13** 0501

[3] Tian Z S, Wang Q, Li Z Q and Wang Y S 2001 *Acta Phys. Sin.* **50** 2368 (in Chinese)

[4] Youmanns D G 1984 *Appl. Phys. Lett.* **44** 365

[5] Newman L A, Hart Richard A, Heath Archie D and Kennedy John 1986 *Appl. Phys. Lett.* **48** 1701

[6] Bourdet G L 1987 *Appl. Phys.* B **43** 701

[7] Abramshi K M, Colley A D, Baker H J and Hall D R 1992 *Oct. Common.* **90** 61

[8] Onson R E and Tobin M S 1972 *Appl. Phys. Lett.* **20** 508

[9] Hester A N and Abrams R L 1972 *Appl. Phys. Lett.* **21** 576

[10] Xin J G, Zang E J and Wei G H 1994 *Optical Engineering.* **33** 1142

[11] Kaye G W C and Laby T H 1999 *Tables of Physical and Chemical Constants (sixth edition)* (No. 137 Chao yang men nei Street: Beijing World Publishing Company) p164–165